SAND2021-12900C

Modal Testing with Piezoelectric Stack Actuators

Garrett K. Lopp*, David M. Siler, Moheimin Khan, Brian C. Owens
Sandia National Laboratories†
Albuquerque, NM 87185

ABSTRACT

Piezoelectric stack actuators can convert an electrical stimulus into a mechanical displacement, which facilitates their use as a vibration excitation mechanism for modal and vibration testing. Due to their compact nature, they are especially suitable for applications where typical electrodynamic shakers may not be physically feasible, e.g., on small-scale centrifuge/vibration (vibrafuge) testbeds. As such, this work details an approach to extract modal parameters using a distributed set of stack actuators incorporated into a vibrafuge system to provide the mechanical inputs. A derivation that considers a lumped-parameter stack-actuator model shows that the transfer functions relating the mechanical responses to the piezoelectric voltages are in a similar form to conventional transfer functions relating the mechanical responses to mechanical forces, which enables typical curve-fitting algorithms to extract the modal parameters. An experimental application consisted of extracting modal parameters from a simple research structure on the centrifuge's arm excited by the vibrafuge's stack actuators. A modal test that utilized a modal hammer on the same structure with the centrifuge arm stationary produced similar modal parameters as the modal parameters extracted from the combined-environments testing with low-level inertial loading.

Keywords: Piezoelectric Actuators, Modal Parameter Extraction, Modal Testing, Centrifuge, Combined Environments

1 INTRODUCTION

The ability of piezoelectric materials to convert energy between the mechanical and electrical domains enables their use in a broad range of applications such as energy harvesting [1, 2], vibration damping and control [3], structural health monitoring [4], and actuation [5], to name a few. Due to their large force density and minimal moving parts, piezoelectric materials are especially useful for vibration-excitation applications when conventional mechanisms (e.g., electromechanical shakers) are physically infeasible. One such application is the use of piezoelectric stack actuators to impart vibration into a test article situated on the rotating arm of a centrifuge [6]. Other applications consist of using piezoelectric patches as the excitation mechanisms in modal tests, which requires measuring the vibration response of a test article subjected to an applied voltage on each piezoelectric patch [7, 8, 9]. The resulting transfer functions then enable the estimation of the test article's modal parameters using typical modal curve-fitting algorithms.

This paper further develops the use of piezoelectric materials for use in modal testing by utilizing a set of stack actuators as the actuation mechanism. Section 2 provides a derivation of the transfer functions relating the piezoelectric voltage to the vibration response of a test article; this derivation considers a simple lumped-parameter actuator model connected between the test article and mounting system, which provides valuable insight into the generated transfer functions. Section 3 details an experimental application that consists of estimating the modal parameters of a piece of research hardware mounted on the end of a rotating centrifuge arm. This section also details a modal test using a conventional modal hammer which is used as a point of comparison. A companion paper provides an overview of the model updating and analysis of this same test article [10]. Finally, Section 4 discusses the relevant conclusions and potential paths forward.

*Corresponding author: glopp@sandia.gov

†Sandia National Laboratories is a multi-mission laboratory managed and operated by National Technology & Engineering Solutions of Sandia, LLC, a wholly owned subsidiary of Honeywell International Inc., for the U.S. Department of Energy's National Nuclear Security Administration under contract DE-NA0003525. This paper describes objective technical results and analysis. Any subjective views or opinions that might be expressed in the paper do not necessarily represent the views of the U.S. Department of Energy or the United States Government.

2 TRANSFER-FUNCTION DERIVATION

Consider the system in Fig. 1a that represents a set of piezoelectric stack actuators mounted between the test article (System A) and the mounting assembly (System B). Both System A and System B consist of a displacement vector ($\mathbf{x}_A$, $\mathbf{x}_B$), a mass matrix ($\mathbf{M}_A$, $\mathbf{M}_B$), and a stiffness matrix ($\mathbf{K}_A$, $\mathbf{K}_B$). To represent a piezoelectric stack actuator, Fig. 1b shows a lumped-parameter model that consists of two masses connected by a stack of piezoelectric wafers. Following a similar derivation for the stack actuator as supplied in [11], the electromechanical equations of motion that govern the actuator dynamics are

$$\underbrace{\begin{bmatrix} m_{p,1} & 0 & 0 \\ 0 & m_{p,2} & 0 \\ 0 & 0 & 0 \end{bmatrix}}_{\mathbf{M}_p} \begin{Bmatrix} \ddot{x}_{p,1} \\ \ddot{x}_{p,2} \\ \dot{Q}_p \end{Bmatrix} + \underbrace{\begin{bmatrix} k_p^E & -k_p^E & 0 \\ -k_p^E & k_p^E & 0 \\ \theta & -\theta & 1 \end{bmatrix}}_{\mathbf{K}_p^E} \begin{Bmatrix} x_{p,1} \\ x_{p,2} \\ Q_p \end{Bmatrix} = \begin{Bmatrix} -\theta \\ \theta \\ C_p^S \end{Bmatrix} V_p + \begin{Bmatrix} -g_{p,1} \\ g_{p,2} \\ 0 \end{Bmatrix} \tag{1}$$

These equations contain three degrees-of-freedom (DOFs): $x_{p,1}$ and $x_{p,2}$ are the displacements at each end of the actuator and Q_p is the electrical charge. Furthermore, V_p is the voltage applied to the stack, and $g_{p,1}$ and $g_{p,2}$ are the reaction forces at each end of the actuator; $m_{p,1}$ and $m_{p,2}$ are the lumped masses, k_p is the combined stiffness of the piezoelectric stack and mechanical spring, θ is the electromechanical coupling, and C_p is the capacitance of the stack; and the subscripts E and S denote quantities at a constant electric field and strain, respectively. Next, connect System A to System B using a total of N_p actuators and apply compatibility and force equilibrium constraints, which results in the electromechanical equations of motion of the combined system:

$$\begin{aligned} &\begin{bmatrix} \mathbf{M}_A + \sum_{j=1}^{N_p} \mathbf{M}_{p,AA,j} & \mathbf{0} & \mathbf{0} \\ \mathbf{0} & \mathbf{M}_B + \sum_{j=1}^{N_p} \mathbf{M}_{p,BB,j} & \mathbf{0} \\ \mathbf{0} & \mathbf{0} & \mathbf{0} \end{bmatrix} \begin{Bmatrix} \ddot{\mathbf{x}}_A \\ \ddot{\mathbf{x}}_B \\ \ddot{\mathbf{Q}}_p \end{Bmatrix} \\ &+ \begin{bmatrix} \mathbf{K}_A + \sum_{j=1}^{N_p} \mathbf{K}_{p,AA,j}^E & -\sum_{j=1}^{N_p} \mathbf{K}_{p,AB,j}^E & \mathbf{0} \\ -\sum_{j=1}^{N_p} \mathbf{K}_{p,BA,j}^E & \mathbf{K}_B + \sum_{j=1}^{N_p} \mathbf{K}_{p,BB,j}^E & \mathbf{0} \\ \sum_{j=1}^{N_p} \mathbf{\Theta}_{A,j} & -\sum_{j=1}^{N_p} \mathbf{\Theta}_{B,j} & \mathbf{I} \end{bmatrix} \begin{Bmatrix} \mathbf{x}_A \\ \mathbf{x}_B \\ \mathbf{Q}_p \end{Bmatrix} = \begin{bmatrix} -\sum_{j=1}^{N_p} \mathbf{\Theta}_{A,j}^t \\ \sum_{j=1}^{N_p} \mathbf{\Theta}_{B,j}^t \\ \mathbf{C}_p^S \end{bmatrix} \mathbf{V}_p \end{aligned} \tag{2}$$

where $\mathbf{Q}_p$ and $\mathbf{V}_p$ are vectors containing the electrical charges and voltages of each actuator, respectively; $\mathbf{M}_{p,AA,j}$ and $\mathbf{M}_{p,BB,j}$ are the mass contributions of the j^{th} actuator to the connection DOFs of Systems A and B, respectively; $\mathbf{K}_{p,AA,j}^E$, $\mathbf{K}_{p,BB,j}^E$, $\mathbf{K}_{p,AB,j}^E$, and $\mathbf{K}_{p,BA,j}^E$ are the stiffness contributions of the j^{th} actuator to the connection DOFs of Systems A and B with the latter two quantities coupling these two systems together; $\mathbf{\Theta}_{A,j}$ and $\mathbf{\Theta}_{B,j}$ are the matrices containing the electromechanical coupling for the j^{th} actuator; and $\mathbf{C}_p^S$ is a diagonal matrix containing the capacitance of each actuator.

The mechanical portion of these equations shows that the mass of the stack actuators are added to both Systems A and B at the connection DOFs and that the actuator stiffness couples these two systems together. Furthermore, the applied voltage appears as a mechanical force acting on the combined system at these same connection DOFs and with a direction in-line with the actuators. Finally, the electrical portion of these equations relates the current required to drive the stack actuators with the prescribed voltages.

Next, transform the above equations into the modal domain using the transformation

$$\begin{Bmatrix} \mathbf{x}_A \\ \mathbf{x}_B \end{Bmatrix} = \begin{bmatrix} \mathbf{\Phi}_{\text{Tot},A} \\ \mathbf{\Phi}_{\text{Tot},B} \end{bmatrix} \boldsymbol{\eta} \tag{3}$$

where $\mathbf{\Phi}_{\text{Tot}}$ are the mode shapes identified from solving the eigenvalue problem associated with the mechanical portion of Eq. 2. Next, apply this transformation to Eq. 2 to obtain the modal equations of motion:

$$\tilde{\mathbf{M}}\ddot{\boldsymbol{\eta}} + \tilde{\mathbf{C}}\dot{\boldsymbol{\eta}} + \tilde{\mathbf{K}}^E\boldsymbol{\eta} = \underbrace{\left[-\mathbf{\Phi}_{\text{Tot},A}^t \sum_{j=1}^{N_p} \mathbf{\Theta}_{A,j}^t + \mathbf{\Phi}_{\text{Tot},B}^t \sum_{j=1}^{N_p} \mathbf{\Theta}_{B,j}^t \right]}_{\tilde{\mathbf{\Theta}}} \mathbf{V}_p \tag{4}$$

where $\tilde{\mathbf{M}}$ and $\tilde{\mathbf{K}}^E$ are the modal mass and stiffness matrices, $\tilde{\mathbf{C}}$ is the modal damping matrix with quantities obtained from a proportional-damping model, and $\tilde{\mathbf{\Theta}}$ is a matrix of electromechanical coupling quantities

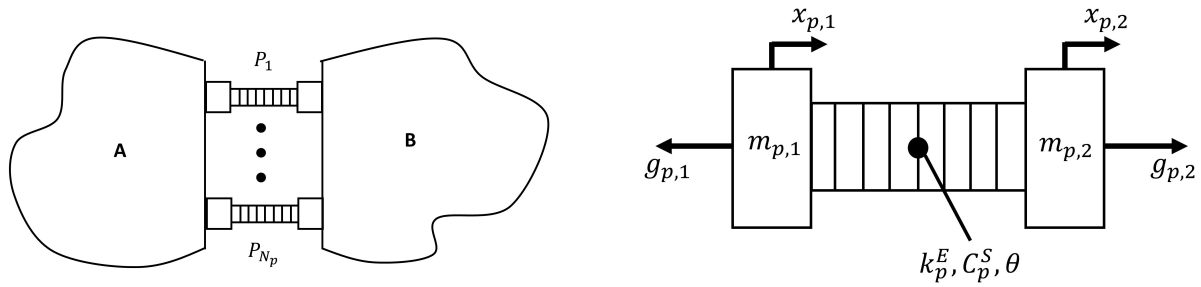

(a) Combined system

(b) Stack actuator

Figure 1: Diagram of a test article excited with piezoelectric stack actuators

corresponding to each mode (rows of the matrix) and each actuator (columns of the matrix). This electromechanical coupling also corresponds to the modal participation factors with respect to the applied voltages. For example, if the electromechanical coupling is large for a given mode and actuator, an applied voltage will significantly excite the mode.

Finally, convert the modal equations to the frequency domain and perform some algebra to obtain the matrix of transfer functions, $\mathbf{H}_{\eta v}$, relating the applied voltages to the modal responses:

$$\boldsymbol{\eta} = \underbrace{\left[\left[\tilde{\mathbf{K}}^E - \omega^2\tilde{\mathbf{M}} + i\omega\tilde{\mathbf{C}}\right]^{-1}\tilde{\boldsymbol{\Theta}}\right]}_{\mathbf{H}_{\eta v}}\mathbf{V}_p \tag{5}$$

For a single mode, this transfer function is

$$H_{\eta v,r,s} = \frac{\eta_r}{V_{p,s}} = \frac{(1/m_r)\tilde{\theta}_{r,s}}{\omega_r^2 - \omega^2 + i2\zeta_r\omega_r\omega} \tag{6}$$

which is similar in form to the transfer functions for a mechanical input, but with the modal electromechanical coupling factors serving as the modal participation factors. As such, typical modal curve-fitting algorithms can estimate the modes of the combined system using the transfer functions relating the voltages to the vibration responses. In many instances, we will prescribe the same voltage, $V_{p,0}$, to each actuator, which reduces the voltage vector to $\mathbf{V}_p = \mathbf{1}V_{p,0}$ and results in the transfer function for a single mode

$$H_{\eta v,r} = \frac{\eta_r}{V_{p,0}} = \frac{(1/m_r)\sum_s^{N_p}\tilde{\theta}_{r,s}}{\omega_r^2 - \omega^2 + i2\zeta_r\omega_r\omega} \tag{7}$$

In this scenario, the modal participation will reduce to zero if the motion at the actuator-connection DOFs for System A and B are the same (e.g., a rigid-body mode), or if the motion at the actuator-connection DOFs for System A and B are equal in magnitude and opposite in sign (e.g., a plate twisting mode with actuators located on each corner).

3 EXPERIMENTAL APPLICATION

To assess the modal-excitation capabilities of piezoelectric stack actuators, we performed an experiment that utilized an array of stack actuators to excite a test article mounted on the end of a rotating centrifuge arm. Figure 2 shows the experimental setup with the test article consisting of an inverted cantilever beam mounted to the fixture housing and with four amplified stack actuators attached between the fixture and centrifuge arm. As the rotation speed of the centrifuge increases, the static inertial loading causes the free end of the beam to contact the housing, thereby altering the mechanical boundary conditions. A common voltage signal, which included either broadband random or a sine sweep, sent to each stack actuator generated vibration at the base of the fixture at several centrifuge rotation speeds, and triaxial accelerometers mounted at various locations on the test article measured the vibration response. A modal test using a conventional modal hammer to excite the test article on a stationary centrifuge arm served as the truth case to compare the modal parameters extracted from the centrifuge rotating at a low speed.

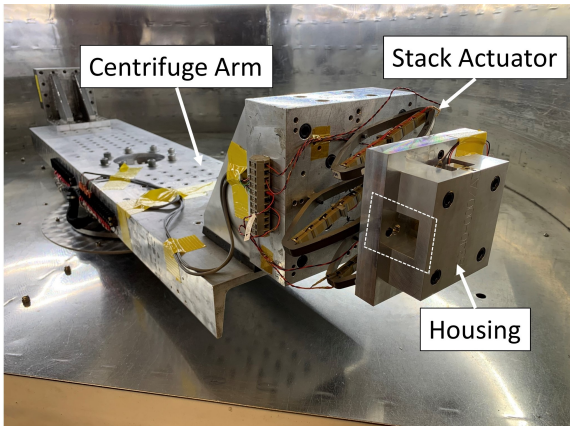

(a) Test article located at the end of the centrifuge arm with the stack actuators supplying the excitation

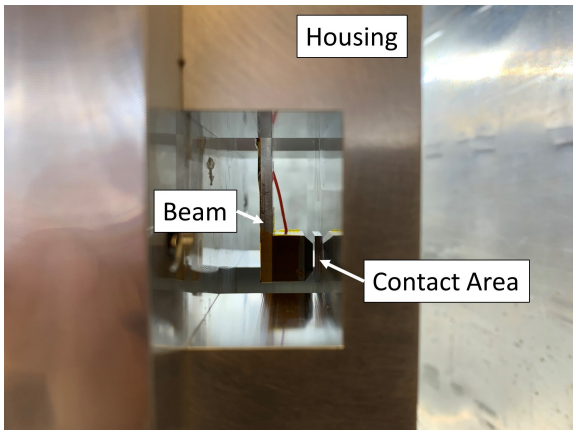

(b) Zoomed-in view of the cantilever beam located in the fixture housing (dashed box in Fig. 2a)

Figure 2: Experimental test setup

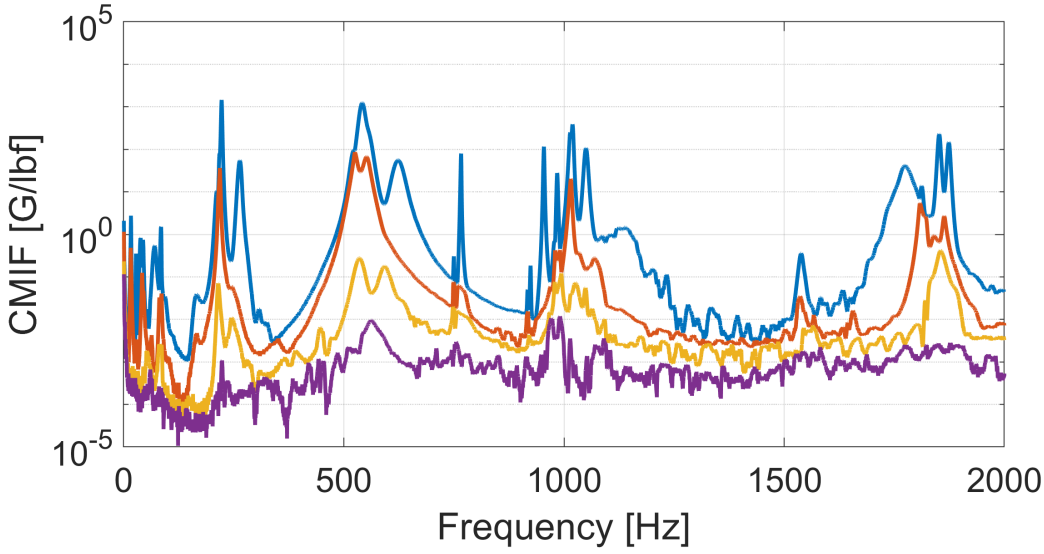

(a) Excitation provided with a modal hammer

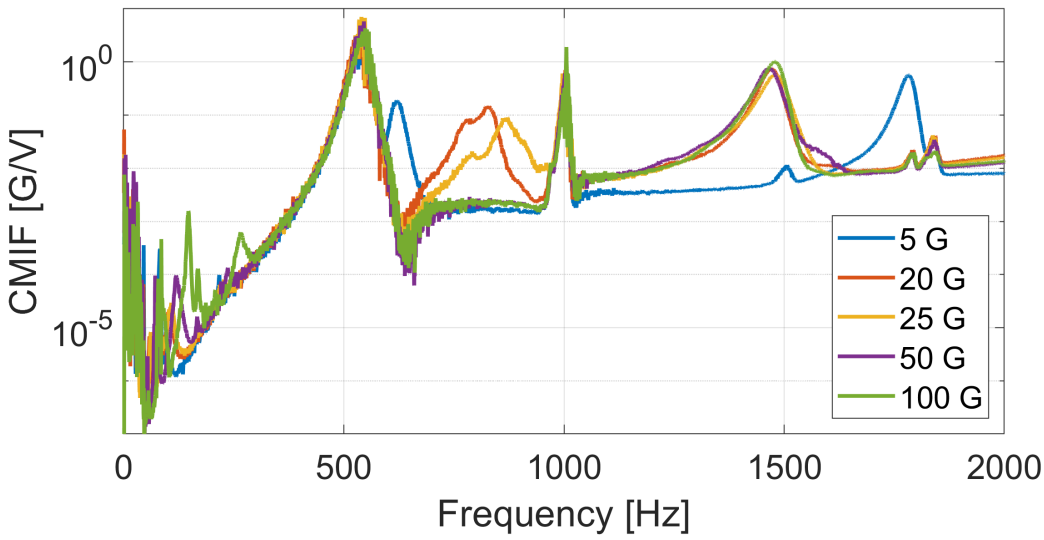

(b) Excitation provided with stack actuators

Figure 3: Complex modal indicator function

Mode Number	Hammer, Freq. [Hz]	Stack, Freq. [Hz]	Freq. Error [%]	Hammer, Damping [%]	Stack, Damping [%]	Damping Error [%]	MAC [%]
1	70.3	75.3	7.2	7.3	6.0	-18.1	82.0
2	84.0	82.8	-1.5	2.0	2.4	20.2	97.9
3	541.8	536.3	-1.0	1.9	2.4	27.5	80.4
4	556.3	549.0	-1.3	2.5	2.5	1.6	99.0
5	623.3	622.8	-0.1	3.3	3.2	-3.4	94.7
6	1019.9	1006.3	-1.3	0.3	0.5	57.4	81.1
7	1775.6	1787.9	0.7	1.2	1.4	14.3	98.0

Table 1: Comparison of modal parameters for the modal hammer and stack actuators

Figure 3a shows a multi-reference complex modal indicator function (CMIF) measured when using the modal hammer to provide the excitation at several locations on the test article, and Fig. 3b shows a single-reference CMIF measured when using the stack actuators to provide the excitation with the centrifuge rotating at various speeds. The response generated from the modal hammer shows a significant increase in modal content compared to that of the stack actuators since these actuators can only excite the modes with significant participation in the actuation direction. Also note that the units are different for both CMIFs, resulting in the CMIF for the stack actuators having peak magnitudes that are much lower than for the hammer. Table 1 shows the modal parameters for the common modes estimated from both excitation strategies. For the stack actuators, this table shows quantities corresponding to the centrifuge rotating at the lowest speed, which generated a static inertial loading of 5 G. For all of these common modes, the frequency error was less than 10% and the MAC was greater than 80%; the damping showed larger discrepancies with errors up to 60%. The modes with MAC values of less than 90% were weakly excited and/or the data was noisy when using the stack actuators, resulting in the discrepancies in the shapes.

Figure 3b also shows that the inertial loading can have a significant effect on some of the test article's modes, which is primarily due to the altered boundary condition associated with the beam tip contacting the housing at higher rotation speeds. At 5 G, the beam tip was not in contact with the housing; however, the tip was in contact with the housing at the larger inertial loadings, resulting in clear frequency shifts for some of the peaks. For example, at 5 G, the first bending mode in the beam's stiff direction, which was tangential to the housing, had a frequency of 270 Hz, and the stack actuators were unable to excite it. At 20 G, the beam tip was in contact with the housing, but still retained a mode of the beam with bending motion tangential to the housing, but with a significant increase in frequency to 829 Hz. At 25 G, the mode with similar motion stiffened further to a frequency of 879 Hz. At 50 G, this mode disappeared entirely. These results suggest that the presence of a contact force when the beam tip contacted the housing resulted in a tangential stiffness that increased as the inertial load and, consequently, the contact force increased. This contact force and tangential stiffness increased until reaching a threshold where it was so large that it prohibited any tangential motion, resulting in a essentially a fixed-fixed boundary condition.

4 CONCLUSIONS

This paper documented the use of piezoelectric stack actuators as the excitation mechanism for modal testing. A derivation of the electromechanical equations of motion for two systems coupled through stack actuators showed that the applied voltage generates a mechanical force acting on the coupled system. This mechanical coupling arises through the actuators linking the two systems together, resulting in the extracted modal parameters corresponding to the coupled system, and not just the test article in isolation. As such, future work will explore methods to decouple the test article from the actuators and downstream system. Finally, the transfer functions relating the applied voltage to the vibration response are in a similar form to the transfer functions measured when using a modal hammer or electrodynamic shaker, enabling the estimation of modal parameters using conventional means.

References

[1] H. Liu, J. Zhong, C. Lee, S.-W. Lee, and L. Lin, "A comprehensive review on piezoelectric energy harvesting technology: Materials, mechanisms, and applications," *Applied Physics Reviews*, vol. 5, no. 041306,

2018.

[2] H. S. Kim, J.-H. Kim, and J. Kim, "A review of piezoelectric energy harvesting based on vibration," *International Journal of Prevision Engineering and Manufacturing*, vol. 12, pp. 1129–1141, 2011.

[3] B. Yan, K. Wang, Z. Hu, C. Wu, and X. Zhang, "Shunt damping vibration control technology: A review," *Applied Sciences*, vol. 7, no. 5, 2017.

[4] W. S. Na and J. Baek, "A review of the piezoelectric electromechanical impedance based structural health monitoring technique for engineering structures," *Sensors*, vol. 18, no. 5, 2018.

[5] Z. Chi and Q. Xu, "International journal of advanced robotic systems," *Recent Advances in the Control of Piezoelectric Actuators*, vol. 11, no. 11, 2014.

[6] D. VanGoethem, R. Jepsen, and E. Romero, "Vibrafuge: Re-entry and launch test simulation in a combined linear acceleration and vibration environment," in *44th AIAA Aerospace Sciences Meeting and Exhibit*, 2012.

[7] W. R. Saunders, D. G. Cole, and H. H. Robertshaw, "Experiments in piezostructure modal analysis for mimo feedback control," *Smart Materials and Structures*, vol. 3, no. 2, 1994.

[8] D. G. Cole, W. R. Saunders, and H. H. Robertshaw, "Modal parameter estimation for piezostructures," *Journal of Vibration and Acoustics*, vol. 117, no. 4, pp. 431–438, 1995.

[9] V. Ruffini, T. Nauman, and C. W. Schwingshackl, "Impulse excitation of piezoelectric patch actuators for modal analysis," in *Topics in Modal Analysis & Testing, Volume 10* (M. Mains and J. R. Blough, eds.), pp. 97–106, Springer International Publishing, 2017.

[10] M. Khan, D. M. Siler, G. K. Lopp, and B. C. Owens, "Model validation for combined inertial acceleration and vibration environments." Paper to be presented at the 40th International Modal Analysis Conference, February 2022.

[11] L. R. Corr and W. W. Clark, "Comparison of low-frequency piezoelectric switch shunt techniques for structural damping," *Smart Materials and Structures*, vol. 11, no. 3, 2002.